

AIP

Conference Proceedings

[HOME](#)[BROWSE](#)[MORE ▾](#)

To support global research during the COVID-19 pandemic, [AIP Publishing is making our content freely available](#) to scientists who register on Scitation.

To gain access, please [log in](#) or [create an account](#) and then [click here](#) to activate your free access. You must be logged in to Scitation to activate your free access.

[Home](#) > [AIP Conference Proceedings](#) > [Volume 1945, Issue 1](#) > [10.1063/1.5030229](#)

[< PREV](#)[NEXT >](#) No Access

Published Online: 03 April 2018

Porous silica nanoparticles as carrier for curcumin delivery

AIP Conference Proceedings 1945, 020007 (2018);

<https://doi.org/10.1063/1.5030229>Sandy Budi Hartono^{1,a)}, Lannie Hadisoewignyo², Wenny Irawaty¹, Luciana Trisna¹, and Robby Wijaya¹[View Affiliations](#)**Topics ▾**

PDF



E-READER

ABSTRACT

Mesoporous silica nanoparticles (MSN) with large surface areas and pore volumes show great potential as drug and gene carriers. However, there are still some challenging issues hinders their clinical application. Many types of research in the use of mesoporous silica material for drug and gene delivery involving complex and rigorous procedures. A facile and reproducible procedure to prepare combined drug carrier is required. We investigated the effect of physiochemical parameters of mesoporous silica, including structural symmetry (cubic and hexagonal), particles size (micro size: 1-2 μm and nano size: 100 -300 nm), on the solubility and release profile of curcumin. Transmission Electron Microscopy, X-Ray Powder Diffraction, and Nitrogen sorption were used to confirm the synthesis of the mesoporous silica materials. Mesoporous silica materials with different mesostructures and size have been synthesized successfully. Curcumin has anti-oxidant, anti-inflammation and anti-virus properties which are beneficial to fight various diseases such as diabetic, cancer, allergic, arthritis and Alzheimer. Curcumin has low solubility which minimizes its therapeutic effect. The use of nanoporous material to carry and release the loaded molecules is expected to enhance curcumin solubility. Mesoporous silica materials with a cubic mesostructure had a higher release profile and curcumin solubility, while mesoporous silica materials with a particle size in the range of nano meter (100-300) nm also show better release profile and solubility.

REFERENCES

(2014). <https://doi.org/10.1039/C3RA44257H>, [Google Scholar](#), [Crossref](#)

2.

Chen AM, Zhang M, Wei D, Stueber D, Taratula O, Minko T, *et al.*, *Small* **5**,2673–2677 (2009). <https://doi.org/10.1002/sml.200900621>, [Google Scholar](#), [Crossref](#)

3.

Amirali Popat SBH, Frances Stahr, Jian Liu, Shi Zhang Qiao and Gao Qing (Max) Lu, *Nanoscale* **3**,2801–2818 (2011). <https://doi.org/10.1039/c1nr10224a>, [Google Scholar](#), [Crossref](#)

4.

Lebold T, Jung C, Michaelis J, Braeuchle C, *Nano Lett* **9**,2877–2883 (2009). <https://doi.org/10.1021/nl9011112>, [Google Scholar](#), [Crossref](#)

5.

Shen J, He Q, Gao Y, Shi J, Li Y, *Nanoscale* **3**,4314–4322 (2011). <https://doi.org/10.1039/c1nr10580a>, [Google Scholar](#), [Crossref](#)

6.

Anand P, Kunnumakkara AB, Newman RA, Aggarwal BB, *Mol Pharmaceutics* **4**,807–818 (2007). <https://doi.org/10.1021/mp700113r>, [Google Scholar](#), [Crossref](#)

7.

Gautam Sethi BSA BBA. “The Role of Curcumin in Modern Medicine” in

 PDF |  E-READER

Ramawat (German: Springer; 2009), pp 97–114. [Google Scholar](#)

8.

Leila Ma'mani SN, Hamidreza Kheiri-manjili, Sharafaldin al-Musawi,,
Mina Saeedi SA, Alireza Foroumadi, Abbas Shafiee, European Journal of
Medicinal Chemistry **83**,646–654 (2014).

<https://doi.org/10.1016/j.ejmech.2014.06.069>, [Google Scholar](#), [Crossref](#)

9.

Stefan Datz HE, Constantin v. Schirnding, Linh Nguyen, Thomas Bein,
Microporous and Mesoporous Materials **225**,371–377 (2016).

<https://doi.org/10.1016/j.micromeso.2016.01.022>, [Google Scholar](#),
[Crossref](#)

10.

Ahmed A, Hearn J, Abdelmagid W, Zhang H, J Mater Chem **22**, 25027–
25035 (2012). <https://doi.org/10.1039/c2jm35569h>, [Google Scholar](#),

[Crossref](#)

11.

Beck JS, JACS **114**,10834–10843 (1992).

<https://doi.org/10.1021/ja00053a020>, [Google Scholar](#), [Crossref](#)

12.

Dongyuan Zhao JF, Qisheng Huo, Nicholas Melosh, Glenn H.

Fredrickson, Bradley F. Chmelka, Galen D. Stucky, Science **279**,548–552
(1998). <https://doi.org/10.1126/science.279.5350.548>, [Google Scholar](#),

13.

Han Y, Ying JY, *Angewandte Chemie International Edition* **44**,288–292 (2005). <https://doi.org/10.1002/anie.200460892>, [Google Scholar](#), [Crossref](#)

14.

Yanzhuo Zhang JW, Xiaoyu Bai, Tongying Jiang, Qiang Zhang, and Siling Wang, *Molecular Pharmaceutics* **9**,505–513 (2012). <https://doi.org/10.1021/mp200287c>, [Google Scholar](#), [Crossref](#)

15.

Fan J, Yu C, Lei J, Zhang Q, Li T, Tu B, *et al.*, *Journal of the American Chemical Society* **127**, 10794–10795 (2005). <https://doi.org/10.1021/ja052619c>, [Google Scholar](#), [Crossref](#)

16.

Sandy Budi Hartono, Lannie Hadisoewignyo, Yanan Yang, Anand Kumar Meka, Antaresti and Chengzhong Yu, *Nanotechnology* **27**,1–7 (2016). <https://doi.org/10.1088/0957-4484/27/50/505605>, [Google Scholar](#), [Crossref](#)

17.

Sasikala Sundar RM, *Shakkthivel Piraman Powder Technology* **266**,321–328 (2014). <https://doi.org/10.1016/j.powtec.2014.06.033>, [Google Scholar](#), [Crossref](#)

M. MATHIAS VA, C.O. ALFARI, F. DALAS, V. CAUDA, M. COMMA,, M.R. DEIGAUO

MV-R, Chemical Engineering Journals **137**,30–37 (2008).

<https://doi.org/10.1016/j.cej.2007.07.078>, [Google Scholar](#), [Crossref](#)

19.

S.W. Song KH, S. Kawi, Langmuir **21**, 9568–9575 (2005).

<https://doi.org/10.1021/la051167e>, [Google Scholar](#), [Crossref](#)

20.

Vishnu Sravan Bollu AKB, Sujan Kumar Mondala, Sanjiv Prasharb,
Mariano Fajardob, David Brionesc, Antonio Rodríguez-Diéguezc, Chitta
Ranjan Patraa, Santiago Gómez-Ruizb,, Materials Science and
Engineering: C **63**, 393–409 (2016)

<https://doi.org/10.1016/j.msec.2016.03.011>, [Google Scholar](#), [Crossref](#)

Published by AIP Publishing.



Resources

AUTHOR

[↓](#) PDF | [📄](#) E-READER

LIBRARIAN

ADVERTISER

General Information

ABOUT

CONTACT

HELP

PRIVACY POLICY

TERMS OF USE

FOLLOW AIP PUBLISHING:



Website © 2020 AIP Publishing LLC.

Article copyright remains as
specified within the article.

Scitation



AIP Conference Proceedings

HOME

BROWSE

MORE ▼

To support global research during the COVID-19 pandemic, [AIP Publishing is making our content freely available](#) to scientists who register on Scitation.

To gain access, please [log in](#) or [create an account](#) and then [click here](#) to activate your free access. You must be logged in to Scitation to activate your free access.

• Table of Contents

PROCEEDINGS OF THE 3RD INTERNATIONAL CONFERENCE ON MATERIALS AND METALLURGICAL ENGINEERING AND TECHNOLOGY (ICOMMET 2017): Advancing Innovation in Materials Science, Technology and Applications for Sustainable Future

< PREV NEXT >



Conference date: 30–31 October 2017

Location: Surabaya, Indonesia

ISBN: 978-0-7354-1640-6

Editors: Mas Irfan P. Hidayat

Volume number: 1945

Published: Apr 3, 2018

DISPLAY : 20 50 100 all

BROWSE VOLUMES

PRELIMINARY



No Access . April 2018

Preface: Proceedings of the 3rd International Conference on Materials and Metallurgical Engineering and Technology (ICOMET 2017)

AIP Conference Proceedings **1945**, 010001 (2018); <https://doi.org/10.1063/1.5030221>



No Access . April 2018

Program Committees: Proceedings of the 3rd International Conference on Materials and Metallurgical Engineering and Technology (ICOMET 2017)

AIP Conference Proceedings **1945**, 010002 (2018); <https://doi.org/10.1063/1.5030222>



No Access . April 2018

List of Keynote Talks: Proceedings of the 3rd International Conference on Materials and Metallurgical Engineering and Technology (ICOMET 2017)

AIP Conference Proceedings **1945**, 010003 (2018); <https://doi.org/10.1063/1.5031704>



CONTRIBUTED ORAL PAPERS

BROWSE VOLUMES



No Access . April 2018

Effect of drug loading method against drug dissolution mechanism of encapsulated amoxicillin trihydrate in matrix of semi-IPN chitosan-poly(*N*-vinylpyrrolidone) hydrogel with KHCO_3 as pore forming agent in floating drug delivery system

Khansa Fimantari and Emil Budianto

AIP Conference Proceedings **1945**, 020001 (2018); <https://doi.org/10.1063/1.5030223>

SHOW ABSTRACT



No Access . April 2018

Effects of pore forming agents of potassium bicarbonate and drug loading method against dissolution mechanisms of amoxicillin drugs encapsulated in hydrogel full-Ipn chitosan-poly(*N*-vinylcaprolactam) as a floating drug delivery system

Nurul Aini, Dyah Utami Cahyaning Rahayu and Emil Budianto

AIP Conference Proceedings **1945**, 020002 (2018); <https://doi.org/10.1063/1.5030224>

SHOW ABSTRACT




No Access . April 2018

Effect of drug loading method against the dissolution mechanism of encapsulated amoxicillin trihydrate drug in matrix of semi-IPN chitosan-poly (*N*-vinyl pyrrolidone) hydrogel with pore forming agent CaCO_3

Yanah Nurjannah and Emil Budianto

AIP Conference Proceedings **1945**, 020003 (2018); <https://doi.org/10.1063/1.5030225>

BROWSE VOLUMES

[SHOW ABSTRACT](#) No Access . April 2018

The effects of honey (*Apis dorsata*) supplements on increased bone strength in ovariectomized rat as animal model of osteoporosis

Ira Sari Yudaniayanti, Hardany Primarizky and Lianny Nangoi

AIP Conference Proceedings **1945**, 020004 (2018); <https://doi.org/10.1063/1.5030226>

[SHOW ABSTRACT](#) No Access . April 2018

Comparison electrical stimulation and passive stretching for blood glucose control type 2 diabetes mellitus patients

Rika Wahyuni Arsianti, Dewy Haryanti Parman and Hendy Lesmana

AIP Conference Proceedings **1945**, 020005 (2018); <https://doi.org/10.1063/1.5030227>

[SHOW ABSTRACT](#) No Access . April 2018

Blood plasma separation in ZnO nanoflowers-supported paper based microfluidic for glucose sensing

Luthviah Choirotul Muhimmah, Roekmono, Harsono Hadi, Rio Akbar Yuwono and Ruri Agung Wahyuono

AIP Conference Proceedings **1945**, 020006 (2018); <https://doi.org/10.1063/1.5030228>

[SHOW ABSTRACT](#)[BROWSE VOLUMES](#)



No Access . April 2018

Porous silica nanoparticles as carrier for curcumin delivery

Sandy Budi Hartono, Lannie Hadisoewignyo, Wenny Irawaty, Luciana Trisna and Robby Wijaya

AIP Conference Proceedings **1945**, 020007 (2018); <https://doi.org/10.1063/1.5030229>

SHOW ABSTRACT



No Access . April 2018

Effect of deposition time of sputtering Ag-Cu thin film on mechanical and antimicrobial properties

A. Purniawan, R. Hermastuti, H. Purwaningsih and T. M. Atmono

AIP Conference Proceedings **1945**, 020008 (2018); <https://doi.org/10.1063/1.5030230>

SHOW ABSTRACT



No Access . April 2018

Morphology and inhibition performance of Ag thin film as antimicrobial coating deposited by RF-PVD on 316 L stainless steel

A. Purniawan, Y. S. A. Khrisna, A. Rasyida and T. M. Atmono

AIP Conference Proceedings **1945**, 020009 (2018); <https://doi.org/10.1063/1.5030231>

SHOW ABSTRACT



BROWSE VOLUMES

Influence of copper composition on mechanical properties of biodegradable material Mg-Zn-Cu for orthopedic application

A. Purniawan, H. M. Maulidiah and H. Purwaningsih

AIP Conference Proceedings **1945**, 020010 (2018); <https://doi.org/10.1063/1.5030232>

SHOW ABSTRACT



 No Access . April 2018

Pin on flat wear volume prediction of UHMWPE against cp Ti for orthopedic applications

Handoko, Suyitno, Rini Dharmastiti and Rahadyan Magetsari

AIP Conference Proceedings **1945**, 020011 (2018); <https://doi.org/10.1063/1.5030233>

SHOW ABSTRACT



 No Access . April 2018

Characterization of biocomposites of sheep hydroxyapatite (SHA)/shellac/sugar as bone filler material

Joko Triyono, Yushak Rizha and Teguh Triyono

AIP Conference Proceedings **1945**, 020012 (2018); <https://doi.org/10.1063/1.5030234>

SHOW ABSTRACT



 No Access . April 2018

Cytotoxic activity of ethanolic extract of the marine sponge *Aaptos suberitoides* against T47D cell


Awik Dwi Diah Nurhayati, Parastoeti Prastiwi, Sukardiman and Tri Wahyuningsih

[BROWSE VOLUMES](#)

AIP Conference Proceedings **1945**, 020013 (2018); <https://doi.org/10.1063/1.5030235>

SHOW ABSTRACT



 No Access . April 2018

Effect drug loading process on dissolution mechanism of encapsulated amoxicillin trihydrate in hydrogel *semi*-IPN chitosan methyl cellulose with pore forming agent KHCO_3 as a floating drug delivery system

Garnis Fithawati and Emil Budianto

AIP Conference Proceedings **1945**, 020014 (2018); <https://doi.org/10.1063/1.5030236>

SHOW ABSTRACT



 No Access . April 2018


Preparation and characterization of porous Mg-Zn-Ca alloy by space holder technique

D. Annur, Franciska P. Lestari, A. Erryani, Fernando A. Sijabat, I. N. G. P. Astawa and I. Kartika

AIP Conference Proceedings **1945**, 020015 (2018); <https://doi.org/10.1063/1.5030237>

SHOW ABSTRACT



 No Access . April 2018

Effects of pore CaCO_3 form agencies on dissolution mechanisms of amoxicillin drugs encapsulated in hydrogels *semi*-IPN chitosan Methyl cellulose

[BROWSE VOLUMES](#)

Emil Budianto and Maghfira Fauzia

AIP Conference Proceedings **1945**, 020016 (2018); <https://doi.org/10.1063/1.5030238>

SHOW ABSTRACT



 No Access . April 2018


Determination of elastic modulus of ceramics using ultrasonic testing

Firmansyah Sasmita, Gatot Wibisono, Hermawan Judawisastra and Toni Agung Priambodo

AIP Conference Proceedings **1945**, 020017 (2018); <https://doi.org/10.1063/1.5030239>

SHOW ABSTRACT



 No Access . April 2018

Numerical simulation of temperature distribution in cylindrical ilmenite (FeTiO_3) due to microwave heating

Mas Irfan P. Hidayat, Dian Mughni Fellicia and Ferdiansyah Iqbal Rafandi

AIP Conference Proceedings **1945**, 020018 (2018); <https://doi.org/10.1063/1.5030240>

SHOW ABSTRACT



 No Access . April 2018

Prediction of composite fatigue life under variable amplitude loading using artificial neural network trained by genetic algorithm

Muhamad Nur Rohman, Mas Irfan P. Hidayat and Agung Purniawan

BROWSE VOLUMES

AIP Conference Proceedings **1945**, 020019 (2018); <https://doi.org/10.1063/1.5030241>

SHOW ABSTRACT



 No Access . April 2018

Simulation of impact ballistic of Cu-10wt%Sn frangible bullet using smoothed particle hydrodynamics

Mas Irfan P. Hidayat, Widyastuti and Peniel Simaremare

AIP Conference Proceedings **1945**, 020020 (2018); <https://doi.org/10.1063/1.5030242>

SHOW ABSTRACT



 No Access . April 2018

Upgrading nickel content of limonite nickel ore through pelletization, selective reduction and magnetic separation

W. Mayangsari, A. B. Prasetyo and Puguh Prasetyo

AIP Conference Proceedings **1945**, 020021 (2018); <https://doi.org/10.1063/1.5030243>

SHOW ABSTRACT



 No Access . April 2018


The effect of temperature and addition of reducing agent on sodium stannate preparation from cassiterite by the alkaline roasting process

Latifa Hanum Lalasari, Lia Andriyah, Tri Arini and F. Firdiyono

AIP Conference Proceedings **1945**, 020022 (2018); <https://doi.org/10.1063/1.5030244>

BROWSE VOLUMES

SHOW ABSTRACT

 No Access . April 2018

The effect of smelting time and composition of palm kernel shell charcoal reductant toward extractive Pomalaa nickel laterite ore in mini electric arc furnace

Iqbal Huda Sihotang, Yayat Iman Supriyatna, Ika Ismail and Sulistijono

AIP Conference Proceedings **1945**, 020023 (2018); <https://doi.org/10.1063/1.5030245>

SHOW ABSTRACT

 No Access . April 2018

Beneficiation of Kulon Progo iron sand by using tabling and magnetic separation methods

Soesaptri Oediyani, Ikhlasul Amal M., M. Victoriyan N. and Andinnie Juniarsih

AIP Conference Proceedings **1945**, 020024 (2018); <https://doi.org/10.1063/1.5030246>

SHOW ABSTRACT

 No Access . April 2018

Nanocellulose based polymer composite for acoustical materials

Mohammad Farid, Agung Purniawan, Diah Susanti, Slamet Priyono, Hosta Ardhyanta and Mutia E. Rahmasita

AIP Conference Proceedings **1945**, 020025 (2018); <https://doi.org/10.1063/1.5030247>

SHOW ABSTRACT



BROWSE VOLUMES



No Access . April 2018

Effects of aluminum and copper chill on mechanical properties and microstructures of Cu-Zn-Al alloys with sand casting

Hosta Ardhyananta, Alvian Toto Wibisono, Mavindra Ramadhani, Widyastuti, Muhammad Farid and Muhammad Shena Gumilang

AIP Conference Proceedings **1945**, 020026 (2018); <https://doi.org/10.1063/1.5030248>

SHOW ABSTRACT



No Access . April 2018

Formation of polycrystalline MgB₂ synthesized by powder in sealed tube method with different initial boron phase

Sigit Dwi Yudanto, Agung Imaduddin, Budhy Kurniawan and Azwar Manaf

AIP Conference Proceedings **1945**, 020027 (2018); <https://doi.org/10.1063/1.5030249>

SHOW ABSTRACT



No Access . April 2018

The effect of Li₂CO₃ substitution on synthesis of LiBOB compounds as salt of electrolyte battery lithium ion

Titik Lestariningsih, Ety Marty Wigayati, Qolby Sabrina, Bambang Prihandoko and Slamet Priyono

AIP Conference Proceedings **1945**, 020028 (2018); <https://doi.org/10.1063/1.5030250>

SHOW ABSTRACT



BROWSE VOLUMES



No Access . April 2018

Towards better light harvesting capability for DSSC (dye sensitized solar cells) through addition of Au@SiO₂ core-shell nanoparticles

Nur Fadhilah, Emha Riyadhul Jinan Alhadi and Doty Dewi Risanti

AIP Conference Proceedings **1945**, 020029 (2018); <https://doi.org/10.1063/1.5030251>

SHOW ABSTRACT



No Access . April 2018

Fabrication of MgB₂ monofilament wire by in-situ using powder-in-tube (PIT) method

Muhammad Emir Hanif Rasyadi, Sigit Dwi Yudanto, Agung Imaduddin and Dyah Sawitri

AIP Conference Proceedings **1945**, 020030 (2018); <https://doi.org/10.1063/1.5030252>

SHOW ABSTRACT



No Access . April 2018

Multimode-singlemode-multimode optical fiber sensor coated with novolac resin for detecting liquid phase alcohol

Marfu'ah, Niza Rosyda Amalia, Agus Muhamad Hatta and Detak Yan Pratama

AIP Conference Proceedings **1945**, 020031 (2018); <https://doi.org/10.1063/1.5030253>

SHOW ABSTRACT



No Access . April 2018

BROWSE VOLUMES


Study of crystallization kinetics of peek thermoplastics using Nakamura equation

Mochamad Chalid, Muhammad Joshua Y. B., Arbi Irsyad Fikri, Noel Gregory, Dedi Priadi and Jaka Fajar Fatriansyah

AIP Conference Proceedings **1945**, 020032 (2018); <https://doi.org/10.1063/1.5030254>

SHOW ABSTRACT



 No Access . April 2018


Analysis of holding time variations to Ni and Fe content and morphology in nickel laterite limonitic reduction process by using coal-dolomite bed

Fakhreza Abdul, Sungging Pintowantoro and Ridwan Bagus Yuwandono

AIP Conference Proceedings **1945**, 020033 (2018); <https://doi.org/10.1063/1.5030255>

SHOW ABSTRACT



 No Access . April 2018

Effects of reduction temperature to Ni and Fe content and the morphology of agglomerate of reduced laterite limonitic nickel ore by *coal-bed* method

Fakhreza Abdul, Sungging Pintowantoro, Adji Kawigraha and Ahlidin Nursidiq

AIP Conference Proceedings **1945**, 020034 (2018); <https://doi.org/10.1063/1.5030256>

SHOW ABSTRACT



 No Access . April 2018

BROWSE VOLUMES

Study of variation grain size in desulfurization process of calcined petroleum coke

Sungging Pintowantoro, Muhammad Arif Setiawan and Fakhreza Abdul

AIP Conference Proceedings **1945**, 020035 (2018); <https://doi.org/10.1063/1.5030257>

SHOW ABSTRACT



No Access . April 2018

The effect of BaM/PANI composition with epoxy paint matrix on single and double layers coating with spray coating method for radar absorbing materials applications

Widyastuti, Rindang Fajarin, Vania Mitha Pratiwi, Rifki Rachman Kholid and Abdulloh Habib

AIP Conference Proceedings **1945**, 020036 (2018); <https://doi.org/10.1063/1.5030258>

SHOW ABSTRACT



No Access . April 2018

The effect of milling time and sintering temperature on Mn, Ti substituted barium hexaferrite nanoparticle

Erlina Yustanti and Azwar Manaf

AIP Conference Proceedings **1945**, 020037 (2018); <https://doi.org/10.1063/1.5030259>

SHOW ABSTRACT



No Access . April 2018

Crystallization kinetics of Pd-based amorphous alloy

BROWSE VOLUMES

AIP Conference Proceedings **1945**, 020038 (2018); <https://doi.org/10.1063/1.5030260>

SHOW ABSTRACT



 No Access . April 2018

Effect of cellulose nanocrystals (CNC) addition and citric acid as co-plasticizer on physical properties of sago starch biocomposite

Halimatuddahlia Nasution, Yayang Afandy and M. Thoriq Al-fath

AIP Conference Proceedings **1945**, 020039 (2018); <https://doi.org/10.1063/1.5030261>

SHOW ABSTRACT



 No Access . April 2018

Synthesis of green Fe³⁺/glucose/rGO electrode for supercapacitor application assisted by chemical exfoliation process from burning coconut shell

Gilang B. A. Putra, Herdy Y. Pradana, Dimas E. T. Soenaryo, Malik A. Baqiya and Darminto

AIP Conference Proceedings **1945**, 020040 (2018); <https://doi.org/10.1063/1.5030262>

SHOW ABSTRACT



 No Access . April 2018


The effect of alkaline treatment and fiber orientation on impact resistant of bio-composites *Sansevieria trifasciata* fiber/polypropylene as automotive components material

BROWSE VOLUMES

AIP Conference Proceedings **1945**, 020041 (2018); <https://doi.org/10.1063/1.5030263>

SHOW ABSTRACT



 No Access . April 2018

Dielectric loss property of strong acids doped polyaniline (PANi)

Rianti Amalia, Mas Ayu Elita Hafizah, Andreas and Azwar Manaf

AIP Conference Proceedings **1945**, 020042 (2018); <https://doi.org/10.1063/1.5030264>

SHOW ABSTRACT



 No Access . April 2018

Phase and crystallite size analysis of (Ti_{1-x}Mo_x)C-(Ni,Cr) cermet obtained by mechanical alloying

Suryana, Muhammad Anis and Azwar Manaf

AIP Conference Proceedings **1945**, 020043 (2018); <https://doi.org/10.1063/1.5030265>

SHOW ABSTRACT



 No Access . April 2018


Release rate of diazinon from microcapsule based on melamine formaldehyde

Noviana Utami C. S. and Rochmadi

AIP Conference Proceedings **1945**, 020044 (2018); <https://doi.org/10.1063/1.5030266>

BROWSE VOLUMES

SHOW ABSTRACT


 No Access . April 2018

Investigation of column flotation process on sulphide ore using 2-electrode capacitance sensor: The effect of air flow rate and solid percentage

Didied Haryono, Sri Harjanto, Rifky Wijaya, Soesaptri Oediyani, Harisma Nugraha, Mahfudz Al Huda and Warsito Purwo Taruno

AIP Conference Proceedings **1945**, 020045 (2018); <https://doi.org/10.1063/1.5030267>

SHOW ABSTRACT


 No Access . April 2018

Sintering temperature effect on electrical and thermal properties of $Zn_{1-x}Al_xO$ as thermoelectric material candidate

Rindang Fajarin, Amelthia Rahel and Widyastuti

AIP Conference Proceedings **1945**, 020046 (2018); <https://doi.org/10.1063/1.5030268>

SHOW ABSTRACT

 No Access . April 2018

Characterization of refractory brick based on local raw material from Lampung Province – Indonesia

Muhammad Amin, Yayat I. Suryana, Kusno Isnugroho, Bramantyo B. Aji, David C. Birawidha and Yusup Hendronursito

AIP Conference Proceedings **1945**, 020047 (2018); <https://doi.org/10.1063/1.5030269>

BROWSE VOLUMES

[1](#) [2](#) >



AIP Conference Proceedings
**The 18th International Conference
on Positron Annihilation**

[ORDER PRINT EDITION](#)

Resources

[AUTHOR](#)

[LIBRARIAN](#)

[ADVERTISER](#)

General Information

[ABOUT](#)

[CONTACT](#)

[HELP](#)

[PRIVACY POLICY](#)

[TERMS OF USE](#)

FOLLOW AIP PUBLISHING:



[BROWSE VOLUMES](#)

Website © 2020 AIP Publishing LLC.

Article copyright remains as
specified within the article.

Scitation

BROWSE VOLUMES

Porous Silica Nanoparticles as Carrier for Curcumin Delivery

Sandy Budi Hartono^{1,a)}; Lannie Hadisoewignyo²; Wenny Irawaty¹; Luciana Trisna¹; and Robby Wijaya¹

¹ *Department of Chemical Engineering, Widya Mandala Catholic University Surabaya, Indonesia*

² *Faculty of Pharmacy, Widya Mandala Catholic University Surabaya, Indonesia*

^{a)}Corresponding author: sandy@ukwms.ac.id

Abstract. Mesoporous silica nanoparticles (MSN) with large surface areas and pore volumes show great potential as drug and gene carriers. However, there are still some challenging issues hinders their clinical application. Many types of research in the use of mesoporous silica material for drug and gene delivery involving complex and rigorous procedures. A facile and reproducible procedure to prepare combined drug carrier is required. We investigated the effect of physiochemical parameters of mesoporous silica, including structural symmetry (cubic and hexagonal), particles size (micro size: 1-2 μm and nano size: 100 -300 nm), on the solubility and release profile of curcumin. Transmission Electron Microscopy, X-Ray Powder Diffraction, and Nitrogen sorption were used to confirm the synthesis of the mesoporous silica materials. Mesoporous silica materials with different mesostructures and size have been synthesized successfully. Curcumin has anti-oxidant, anti-inflammation and anti-virus properties which are beneficial to fight various diseases such as diabetic, cancer, allergic, arthritis and Alzheimer. Curcumin has low solubility which minimizes its therapeutic effect. The use of nanoporous material to carry and release the loaded molecules is expected to enhance curcumin solubility. Mesoporous silica materials with a cubic mesostructure had a higher release profile and curcumin solubility, while mesoporous silica materials with a particle size in the range of nano meter (100-300) nm also show better release profile and solubility.

Keywords. Mesoporous silica materials, nanoparticles, curcumin, solubility and release profile.

INTRODUCTION

In recent decades, there are a large number of researches in exploring the use of mesoporous silica materials in drug and gene delivery (1, 2). Mesoporous silica materials are silica based materials with a pore size between 2 to 50 nm. Based on International Union of Pure and Applied Chemistry (IUPAC) there are three types of porous materials: microporous, mesoporous and macroporous materials. Microporous has a pore size below 2 nm, while macroporous has pore size larger than 50 nm. The very high surface area and pore volume of mesoporous silica materials create much application based on this porous material such as catalysis, chemical synthesis, enzyme immobilization and drug delivery (3). Mesoporous silica materials have also been used to improve the solubility of the drug with low bioavailability such as doxorubicin and paclitaxel (4, 5).

Curcumin has long been known for its anti-oxidant, anti-inflammation and anti-viral properties. These properties are very beneficial for medication of different illness such as diabetes, cancer, allergies, arthritis and Alzheimer's disease. Curcumin has a very low bioavailability which becomes a major concern for its application as medicine (6, 7). Mesoporous silica materials can be used to enhance curcumin solubility. Various approaches have been explored

to use mesoporous silica materials as curcumin carrier (8-10). The approaches are quite complex which make them less practical.

We can simplify the method and make the use of mesoporous silica as carrier more practical, by optimizing the physicochemical properties of mesoporous silica. These properties include surface area, pore size, and particle size. These properties can be adjusted through modification of synthesis parameters. Based on the particle size, MS can be divided into two groups: Mesoporous Silica Micro-particle with size in the range of 1 – 8 μm and Mesoporous Silica Nanoparticle with size below 300 nm (11-13). Zhang *et al.* showed that both silica particles could be used as oral drug carrier or parenteral drug carrier (14).

Herein, we report our study on the effect of physicochemical parameters of mesoporous silica, including structural symmetry (cubic and hexagonal), particles size (micro size: 1-2 μm and nano size: 100 -300 nm), on the solubility and release profile of curcumin.

MATERIALS AND METHODS

Chemicals: Triblock poly(ethylene oxide)-b-poly(propylene oxide)-b-poly(ethylene oxide) copolymer EO₁₀₆PO₇₀EO₁₀₆ (Pluronic F127, MW=13400), copolymer EO₂₀PO₇₀EO₂₀ Pluronic 123, tetraethoxysilane (TEOS, 99%), 1,3,5-trimethylbenzene (TMB), 3-aminopropyl triethoxysilane (APTES 99%), potassium chloride (KCl), phosphate buffer tablet and Tween 80 were purchased from Aldrich. A fluorocarbon surfactant (FC-4) was purchased from Yick-Vic Chemicals & Pharmaceuticals (HK) Ltd. All chemicals were used as received without purification.

Synthesis of Mesoporous silica material with cubic mesostructured in two different particle sizes: Micro size (M-1) and Nano size (N-1)

Micro size (M-1)

Micro size mesoporous silica materials with a cubic mesostructure were synthesized following the previous method by Fan *et al.*(15) with some modification. 1 g of pluronic F127 and 5 g of KCl were mixed in 60 mL of 2 M HCl at 20° C (*synthesis temperature*) and stirred for 30 min. Then, add 1.6 g of TMB and stirring was continued for 6 hours at synthesis temperature. 4 g of TEOS was added and continued stirring for 24 h at 20° C. The solutions after were synthesized then removed to an autoclave and heated at 130° C (*hydrothermal temperature*) for 24 h of hydrothermal treatment. The product was separated, washed and dried. The surfactant is removed by using calcination.

Nano size (N-1)

Nano size mesoporous silica materials with a cubic mesostructure were synthesized following the previous method by Ying *et al.* (13) with some modification. 0.5 g of F127 and 1.4 of FC₄ were mixed in the solutions of 60 mL of 0.02 M HCl for 24 h before 0.5 g of TMB was added and stirring continued for four h, then 3 g of TEOS was mixed into the solutions and was stirred for 24 h at 20° C. The solutions after were synthesized then removed to an autoclave and heated at 130° C (*hydrothermal temperature*) for 24 h of hydrothermal treatment. The product was separated, washed and dried. The surfactant was removed by using calcination

Synthesis of Mesoporous silica material with channel like mesostructured in two different particle sizes: Micro size (M-2) and Nano size (N-2)

Micro size (M-2)

Micro size mesoporous silica materials with a hexagonal mesostructure were synthesized following the previous method by Zhao *et al.* (12) with some modification. 4 g of P123 was added to 100 g water and 7.87 g HCl 37%. The solution is stirred at 35° C overnight. Then, 8.53 g of TEOS was added to solution and stirring was continued for 20 hours. The solution was then placed in an oven at 130° C for 24 hours. The product was separated, washed and dried. The surfactant is removed by using calcination.

Nano size (N-2)

Nano size mesoporous silica materials with a hexagonal mesostructure were synthesized following the previous method by Ying *et al.*(13) with some modification. 0.5 g of P123 and 1.47 g of FC4 were dissolved in 80 mL 0.02 M HCl. 2 g of TEOS was added to the solution and stirred at 35°C for 20 hours. The solution was then placed in an oven at 130°C for 24 hours. The product was separated, washed and dried. The surfactant is removed by using calcination.

APTES modification

Amine functionalization of MS was conducted via grafting method. 0.6 g of mesoporous silica materials was added into 30 ml of Toluene. The mixture was stirred and heated to 70°C. 1.2 ml of APTES was added into the mixture, and the stirring was continued for 20 hours. The product was centrifuged and dried. The products were denoted **M-1A, N-1A, M-2A, and N-2A**.

Curcumin loading, *in vitro* release and solubility test

The loading, release, and solubility test were performed based on the previous method by Jambhrunkar *et al.* with slight modification (1). At first 200 mg of mesoporous silica materials, 50 mg of curcumin and 20 ml of ethanol were mixed and sonicated for 2 min using a bath sonicator. The solution was then placed in a rotary evaporation flask. The temperature of the evaporator was set at 55 °C. At this temperature, ethanol was evaporated slowly under vacuum. Finally, the dry powder was obtained. The *in vitro* release test was conducted by using a dialysis bag method. A mixture of 25 mg of curcumin loaded silica particles, and 5 ml of release solution (phosphate buffered saline (PBS) buffer + 0.8% Tween 80) was placed in the dialysis bag with 14 kDa molecular weight cutoff. The mixture was immersed in 200 ml release solution. At certain interval time, a 1ml of the solution was collected and immediately replaced with 1 ml of release solution. The sample concentration was determined by using a UV-vis spectrophotometer at 432 nm. For the solubility test, an excess of curcumin loaded MS was added into 2 ml of water. The mixture was kept under stirring for 48 h at 37 °C. A supernatant was collected and checked with a UV-vis spectrophotometer at 432 nm.

Characterization

Transmission electron microscopy (TEM) images were obtained by a JEOL 1010 electron microscope with an acceleration voltage 100 kV. Nitrogen sorption isotherms of the samples were obtained using a Quantachrome's Quadrasorb SI analyzer at 77 K. Before the measurements; the samples were degassed overnight at 110 °C in vacuum. The Brumauer-Emmett-Teller (BET) surface area was calculated using experimental points at a relative pressure of $P/P_0 = 0.05-0.25$. The total pore volume was calculated from the N_2 amount adsorbed at the highest P/P_0 ($P/P_0 = 0.99$). For cubic structures, the cavity pore size and entrance pore size are determined from the adsorption and desorption branches, respectively. XRD patterns were collected on a German Bruker D8 Advanced X-Ray Diffractometer with Ni filtered Cu $K\alpha$ radiation (40 kV, 30 mA).

RESULTS AND DISCUSSION

Mesoporous silica materials with different mesostructures (cubic/3D and channel like/2D) and different particle sizes (micro size and nano size) were synthesized. The materials were observed by using TEM. The results can be seen in Figure 1. Fig. 1 A and 1B show material with a cubic mesostructure, while Fig. 1C and 1D display material with a channel like mesostructure. Figure 1A and 1C represent micro size particle. The particle size was around 1- 2 μm . The size of nanoparticles was around 100 nm for N-1 and around 300 nm for N-2 (Fig. 1B and 1D). These sizes are considerably smaller compared to micro size. The TEM images indicate the formation of ordered mesostructures. The typically interconnected pores can be seen from Fig. 1A (15). Fig. 1 C shows a typical pore alignment of a long channel like structures (12). The cubic and channel like structures in nano size silica particles are also obvious (Fig. 1 B and D).

For the nitrogen sorption and XRD analysis of M-1 and N-1, TGA and FTIR analysis of amine functionalized silica, we have reported in our recently published journal (16). Both M-1 and N-1 had a hysteresis of type-H2 that belongs to cubic mesostructure. The pore sizes are similar at 10 nm. Fig. 2 shows the nitrogen sorption analysis for M-2 and N-2. Both materials had a type-H1 hysteresis loop with pore size around 6 nm. The XRD pattern of M-1 and N-1 confirm the formation of cubic structures. The XRD spectra show peaks that can be indexed as 111, 220 and 311 (16). These peaks belong to cubic symmetry. Fig. 3 shows the XRD spectra of M-2 and N-2. There are three peaks that can be indexed as 100,110 and 200. These peaks are associated with hexagonal symmetry.

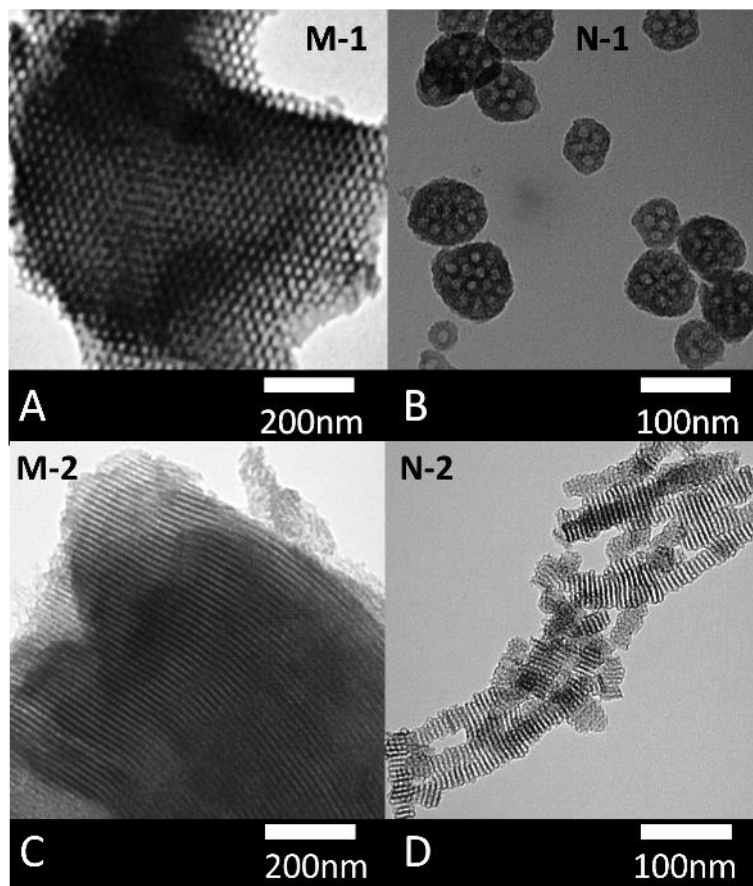


FIGURE 1. TEM images of M-1, N-1, M-2, and N-2.

Amine modified iron nanoparticles have been studied as a carrier of curcumin by Sundar *et al.*(17). However, this study showed that amine functionalized iron oxide nanoparticles had only limited controlled release effect. The system had an issue with a major release of curcumin at an early stage which was caused by the excessive diffusion of curcumin. The main difference between amine-iron oxide nanoparticles and amine-mesoporous silica materials is the presence of the porous network. The porous structure minimizes drug diffusion into the solution. The nanopores within the porous network limits the formation of big particles (aggregates) thus omit the possibilities of excessive drug release. Many studies show the effectiveness of amine functionalization in creating a controlled release profile (18, 19) from mesoporous silica materials. For this reason, the four samples (M-1, N-1, M-2, and N-2) were grafted with amine moieties from APTES.

The amine functionalization materials were characterized by using a Fourier Transform Infrared Spectroscopy (FTIR) and Thermogravimetric Analysis (16). The FTIR analysis confirmed the formation of hydrogen bonding between amine groups and the phenolic hydroxyl group of curcumin. On the basis of TGA analysis, a weight loss of around 18% was found after APTES functionalization.

The loading of curcumin into silica pores was conducted by using the rotary evaporator method. Jambrunkar *et al.* showed (1) that the rotary evaporator method was far more efficient compared to the conventional “physical

mixtures". The method allows better encapsulation of curcumin which causes significant solubility. Fig. 4 shows mesoporous silica nanoparticles and curcumin loaded mesoporous silica materials.

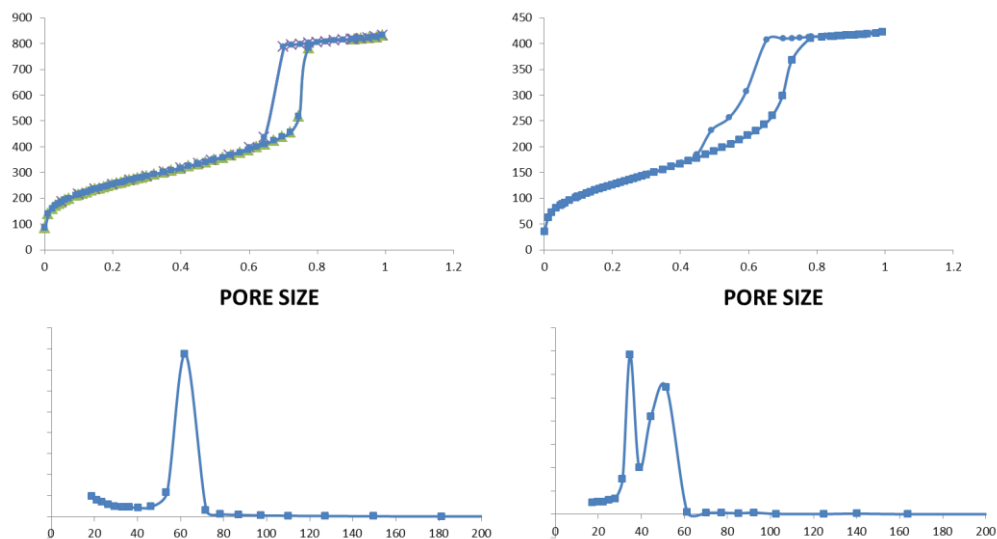


FIGURE 2. Nitrogen sorption analysis and Pore size distribution of M-2 (left) and N-2 (Right)

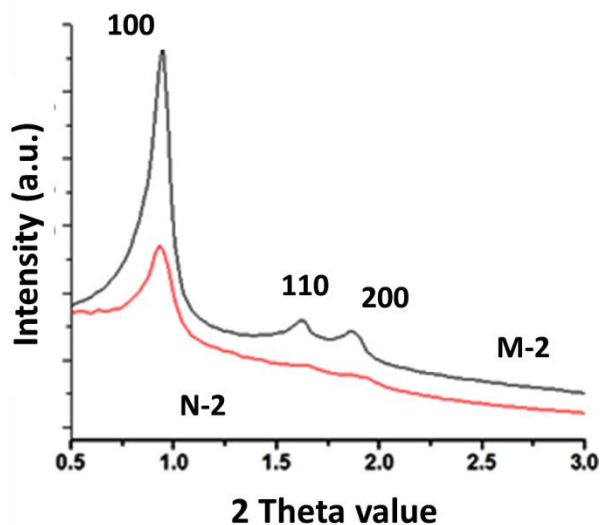


FIGURE 3. XRD spectra of M-2 and N-2.

Fig. 5 shows the *in vitro* release profile for amine functionalized samples (M-2A, N-2A) and free curcumin. Each silica samples had a prolonged release profile. The amount of curcumin release to the media was gradually increased. At the same period, curcumin release from N-2A reached 7% as compared to 5% and 4% for M-2A and free curcumin, respectively. Previously we have reported curcumin release and solubility test results of M-1A and N-1A. The curcumin release from N-1A and M-1A were at around 12% and 9% (16). In general, porous material with cubic structures had a higher release amount of curcumin. In comparison, previous studies by Bollu *et al.* (20) found the release amount of curcumin from amine functionalized MSU-2 (pore size 4.7 nm), and amine functionalized MCM-41 (1.8 nm) were around 8.8% and 1.5%.

The solubility test confirmed that the solubility of curcumin release from N-2A was higher than M-2A and free curcumin. It can be seen that the solubility of curcumin from N-2A was almost four times higher than free curcumin

(Fig. 6). Similar to the *in vitro* release tests, the solubility of curcumin loaded in N-1A and M-1A were higher compared to N-2A and M-2A. The solubility of curcumin from N-1A was ten times as high as the solubility of free curcumin(16). Both tests (release and solubility) informed the superiority of cubic structures samples against channel like structures.

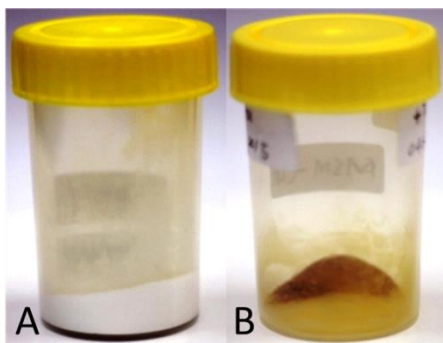


FIGURE 4. Mesoporous silica materials (left) and curcumin loaded mesoporous silica materials (right)

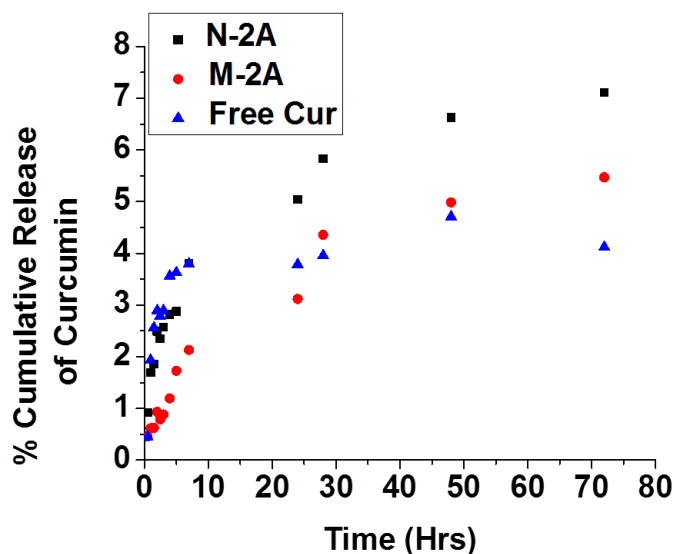


FIGURE 5. The release profile of curcumin from M-2A and N-2A.

Mesostructures (cubic or channel like) and particle size (micro or nano) affect curcumin diffusion within the pores and ultimately influence curcumin release profiles. Firstly, porous materials with three dimension interconnected pores have a better mass transfer and more resistant to pore blockage compared two dimension channel like structures. This is mainly due to its structures in which one main cavity pore is connected with many entrance pores or windows. These entrances guarantee continuing flow of cargo molecules passing through main pores, without having major limitation caused by pore blocking. The pore blocking frequently occurs due to cargo aggregates. Drug powder tends to form aggregates especially at high concentration (4).

Secondly, the particle size determines the effectiveness of mass diffusion. The nano size particles have similar structures with the micro size, but almost ten times smaller in particle size. This short channel determines the distance of drug to move from internal pores to surface. The short channel reduces the steric hindrance from silica walls and enhances the particle release.

The other important factors for interactions between drug molecules and silica particles are the surface functionality. Amine functionalization has been reported effective for a controlled release of curcumin (18, 19). Amine moieties on the silica surface improve the interactions between silica and curcumin. This strong binding

avoids the occurrence of “burst release” of curcumin. The combination of the suitable porous structures and surface functionalization of MSN-A is the underlying reason for the highest solubility of curcumin from N-1A (16).

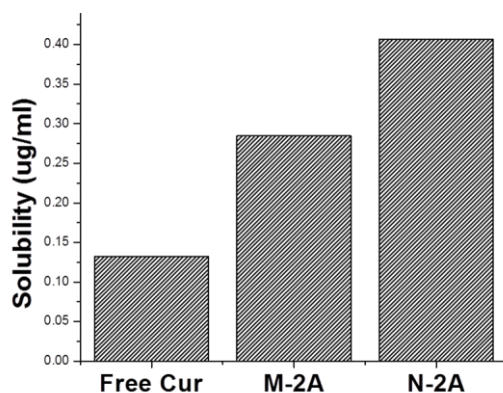


FIGURE 6. The solubility of curcumin from M-2A and N-2A.

CONCLUSION

Despite the obvious benefit from curcumin, the low solubility of these compounds hinders the maximum benefit from curcumin to cure various diseases. Porous silica material with large surface area and pore volume and also tunable pore size is highly effective to increase the solubility of many hydrophobic molecules like curcumin. In summary, a combined curcumin-amine mesoporous silica nanoparticle has been prepared by using a simple approach. This approach improved curcumin in vitro solubility. The improvement of curcumin solubility is very important to enhance its bioavailability which ultimately increases its therapeutic effects that can be very beneficial for treating various diseases such as diabetic and cancer.

ACKNOWLEDGMENTS

We acknowledge the support from Indonesian Directorate General of Higher Education for providing a research grant under the national competition scheme (HIKOM 2015). We are thankful to Prof. Michael Yu and Anand Kumar Meka, Ph.D. from Australian Institute for Bioengineering and Nanotechnology for their generous help in the material characterizations including TEM, nitrogen sorption, and XRD analysis. We also thank the Australian Microscopy and Microanalysis Research Facility at the Centre for Microscopy and Microanalysis, The University of Queensland

REFERENCES

1. Jambhrunkar S, Karmakar S, Popat A, Yu M, Yu C, RSC Adv 4,709-712 (2014).
2. Chen AM, Zhang M, Wei D, Stueber D, Taratula O, Minko T, et al., Small 5,2673-2677 (2009).
3. Amirali Popat SBH, Frances Stahr, Jian Liu, Shi Zhang Qiao and Gao Qing (Max) Lu, Nanoscale 3,2801-2818 (2011).
4. Lebold T, Jung C, Michaelis J, Braeuchle C, Nano Lett 9,2877-2883 (2009).
5. Shen J, He Q, Gao Y, Shi J, Li Y, Nanoscale 3,4314-4322 (2011).
6. Anand P, Kunnumakkara AB, Newman RA, Aggarwal BB, Mol Pharmaceutics 4,807-818 (2007).

7. Gautam Sethi BSaBBA, "The Role of Curcumin in Modern Medicine" in *Herbal Drugs: Ethnomedicine to Modern Medicine*, edited by K.G. Ramawat (German: Springer; 2009), pp 97 - 114.
8. Leila Ma'mani SN, Hamidreza Kheiri-manjili, Sharafaldin al-Musawi,, Mina Saeedi SA, Alireza Foroumadi, Abbas Shafiee, *European Journal of Medicinal Chemistry* 83,646-654 (2014).
9. Stefan Datz HE, Constantin v. Schirnding, Linh Nguyen, Thomas Bein, *Microporous and Mesoporous Materials* 225,371-377 (2016).
10. Ahmed A, Hearn J, Abdelmagid W, Zhang H, *J Mater Chem* 22,25027-25035 (2012).
11. Beck JS, *JACS* 114,10834-10843 (1992).
12. Dongyuan Zhao JF, Qisheng Huo, Nicholas Melosh, Glenn H. Fredrickson, Bradley F. Chmelka, Galen D. Stucky, *Science* 279,548-552 (1998).
13. Han Y, Ying JY, *Angewandte Chemie International Edition* 44,288-292 (2005).
14. Yanzhuo Zhang JW, Xiaoyu Bai, Tongying Jiang, Qiang Zhang, and Siling Wang, *Molecular Pharmaceutics* 9,505-513 (2012).
15. Fan J, Yu C, Lei J, Zhang Q, Li T, Tu B, et al., *Journal of the American Chemical Society* 127,10794-10795 (2005).
16. Sandy Budi Hartono, Lannie Hadisoewignyo, Yanan Yang, Anand Kumar Meka, Antaresti and Chengzhong Yu, *Nanotechnology* 27,1-7 (2016).
17. Sasikala Sundar RM, *Shakthivel Piraman Powder Technology* 266,321-328 (2014).
18. M. Manzano VA, C.O. Are'an, F. Balas, V. Cauda, M. Colilla,, M.R. Delgado MV-R, *Chemical Engineering Journals* 137,30-37 (2008).
19. S.W.Song KH, S.Kawi, *Langmuir* 21,9568-9575 (2005).
20. Vishnu Sravan Bollu AKB, Sujan Kumar Mondala, Sanjiv Prasharb, Mariano Fajardob, David Brionesc, Antonio Rodríguez-Diéguezc, Chitta Ranjan Patraa, Santiago Gómez-Ruizb, , *Materials Science and Engineering: C* 63,393-409 (2016)